Macromolecules
ARTICLE

*Macromolecules* **2009**, *42*, 4237–4243 **4237**
DOI: 10.1021/ma900389n

# Mechanically and Thermally Robust Ordered Nanoporous Monoliths Using Norbornene-Functional Block Polymers

**Liang Chen and Marc A. Hillmyer***

*Department of Chemistry, University of Minnesota, 207 Pleasant Street SE, Minneapolis, Minnesota 55455-0431*

*Received February 19, 2009; Revised Manuscript Received April 15, 2009*

ABSTRACT: A norbornene-functional styrene was synthesized and copolymerized with styrene, and monomer reactivity ratios were calculated in a controlled radical copolymerization. Polylactide-*b*-poly (norbornenylethylstyrene-*s*-styrene) (PLA-*b*-P(N-S)) block polymers were produced by a reversible addition−fragmentation chain transfer polymerization technique using a PLA-based macro chain transfer agent and fully characterized using conventional techniques. Blends composed of this block copolymer, dicyclopentadiene (DCPD), and a metathesis catalyst were waxy materials that formed ordered structures containing cylindrical PLA nanodomains in a composite DCPD/P(N-S) matrix. These composite materials were pressed in a channel die to align the cylindrical domains and were cured by a ring-opening metathesis mechanism at elevated temperatures. Removal of the PLA from the resulting monoliths by mild basic etching resulted in nanoporous monoliths with cylindrical channels. The nanoporous materials were characterized by small-angle X-ray scattering, scanning electron microscopy, and $N_2$ adsorption experiments. The nanoporous monoliths were thermally stable up to about 130 °C and exhibited remarkable mechanical strength that was comparable to pure polyDCPD.

## Introduction

The concept of utilizing self-assembled block copolymer precursors to produce nanoporous structures by selective etching of a sacrificial component has been widely explored in both thin films and monoliths.[1,2] In addition to the utility of nanoporous polymers for templating other nanostructures,[3] applications of such materials as separation membranes[4] and antireflection coatings[5] have been reported. Polylactide (PLA) is a particularly attractive sacrificial block because of the straightforward synthesis of various PLA-containing block copolymers and the susceptibility of PLA to hydrolytic degradation under relatively mild conditions. For example, we have demonstrated that nanoporous polystyrene (PS) monoliths can be prepared from various self-assembled PLA-containing block polymers.[6,7] However, limited thermal stability, intrinsic brittleness, and poor solvent resistance of nanoporous PS has been limiting in template synthesis[8] and separation membrane applications.[4]

Several approaches have been taken to combat the thermal instability of such nanoporous materials. Wolf et al. prepared nanoporous polycyclohexylethylene (PCHE) monoliths from ordered PCHE-*b*-PLA copolymers, which exhibited improved thermal stability to about 140 °C;[9] nanoporous PS collapses around 100 °C.[6] Another approach by Hawker and coworkers involved the thermolysis of benzocyclobutane-modified (BCB) PS-containing block copolymer thin films with polymethylmethacrylate (PMMA) or PLA as a degradable block resulting in enhanced thermal stability in nanoporous thin films.[10] Likewise, cross-linking double bonds in ordered polydimethylsiloxane (PDMS)-*b*-polyisoprene (PI)[11] or PDMS-*b*-polybutadiene (PB)[12] block copolymers having PDMS as a degradable block has been reported to yield good solvent resistance and thermal stability in the resulting monoliths. Additionally, Zhou et al. reported the PI cross-linking using $S_2Cl_2$ in a bicontinuous microemulsion of PS/PS-PI/PI, and after solvent extraction of PS, the resultant nanoporous monoliths were thermally stable to 160 °C. Tensile tests on these monoliths indicated an elongation at break of 2% with a tensile strength of 50 MPa; the relative brittleness of nanoporous monoliths was attributed to extensive cross-linking of the polyisoprene phase.[13]

Whereas improvements in the thermal stability have been achieved, most nanoporous materials templated from ordered block copolymers still suffer from poor mechanical performance. In 2006, Uehara et al. demonstrated that nanoporous semicrystalline polyethylene (PE) membranes derived from a PE−PS block copolymer could be prepared.[14] These materials were particularly tough, and this work was a breakthrough in the development of new nanoporous membranes for separation applications.

Polydicyclopentadiene (polyDCPD) synthesized by ring-opening metathesis polymerization (ROMP) exhibits both a high modulus and a high tensile strength and is therefore an attractive candidate for the matrix material in nanoporous materials derived from block copolymers.[15] In a recent communication, we reported the production of tough 3D continuous nanoporous membranes using PLA-*b*-poly(norbornenylethylstyrene−styrene) (P(N-S)) via polymerization-induced phase separation (PIPS) during the ROMP of DCPD. Those materials exhibited appealing features for membrane applications: high thermal stability and excellent mechanical properties.[16] In this article, we (i) fully address the synthesis and characterization of the monomer *p*-norbornenylethylstyrene (N) and derived PLA-*b*-P(N-*s*-S) block copolymers, (ii) explore the kinetics of the reversible addition−fragmentation chain transfer (RAFT) copolymerization of styrene and N, and (iii) prepare ordered cross-linked nanoporous monoliths using blends of these PLA-*b*-P(N-*s*-S) block copolymers with DCPD and a metathesis catalyst

*To whom correspondence should be addressed. E-mail: hillmyer@umn.edu.

© 2009 American Chemical Society
Published on Web 05/19/2009

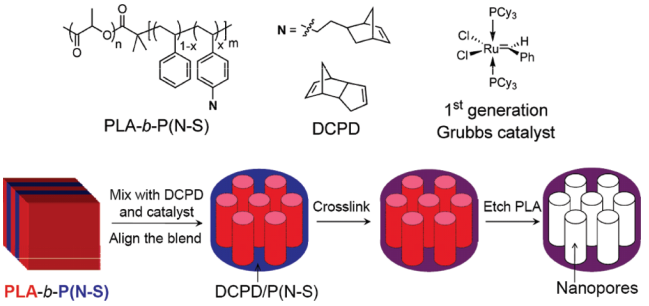


**Figure 1.** Chemical structure of cross-linking components and scheme illustrating fabrication of cross-linked nanoporous monoliths by metathesis reaction.

(as shown schematically in Figure 1). Such nanoporous monoliths with aligned cylindrical pores were thermally robust and mechanically strong and exhibited exceptional solvent resistance. This new method for preparing nanoporous polymers will significantly broaden their applicability.

## Results and Discussion

**Material Synthesis and Characterization** *Monomer Synthesis and Characterization.* 5-Bromomethyl norbornene (mainly the endo isomer) was treated with magnesium in THF to form the corresponding Grignard reagent. In the presence of $Li_2CuCl_4$, this norbornenylmethyl magnesium bromide was coupled to vinylbenzyl chloride at −78 °C to produce the monomer N (Figure 2). The $^{13}C$ NMR and $^1H$ NMR spectra of purified N (Figures S1 and S2 in the Supporting Information) indicate a product of high purity that is consistent with the structure depicted in Figure 2. Infrared spectroscopy, gas chromatography−mass spectrometry, and elemental analysis were corroborative. (See the Experimental Section.)

This new norbornene-containing styrene is amenable to anionic polymerization, which has been widely employed as a robust technique for synthesizing numerous functional styrene monomers.[17] Using *sec*-BuLi as the initiator and a monomer-to-initiator ratio of 40, we synthesized poly (norbornenylethylstyrene) (PN) and isolated it in near quantitative yield. A number-average molecular weight of 6.7 kg mol$^{-1}$ and a narrow polydispersity index (PDI) of 1.04 were determined by size exclusion chromatography (SEC) analysis based on PS standards. The $^1H$ NMR spectrum of this product confirmed complete retention of norbornene groups throughout the polymerization (Figure S1 in the Supporting Information). The glass-transition temperature ($T_g$) of the resulting PN was 81 °C by differential scanning calorimetry (DSC). By the use of anionic polymerization, followed by sequential addition of another monomer or end-capping reaction with ethylene oxide,[18] various norbornene-functional block copolymers can be potentially produced.

*Controlled Free Radical Copolymerization of N and Styrene.* We also explored the copolymerization of N and styrene following a RAFT scheme using a trithiocarbonate as the chain transfer agent.[19] (See the Experimental Section.) We carried out copolymerizations at various feed compositions to low conversion and analyzed the resultant copolymers by $^1H$ NMR spectroscopy to determine the relative amounts of incorporated N and styrene. The overall monomer conversions were determined to be lower than 6 wt % on the basis of the mass of recovered polymers and molecular weight determination through NMR analysis. Specifically, copolymerization reactions were carried out under two

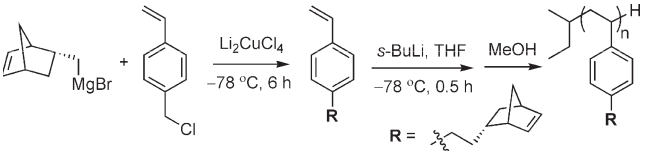


**Figure 2.** Synthesis of *p*-norbornenylethylstyrene (N) via the Grignard reaction and resulting polymer *p*-norbornenylethyl styrene (PN) by anionic polymerization.

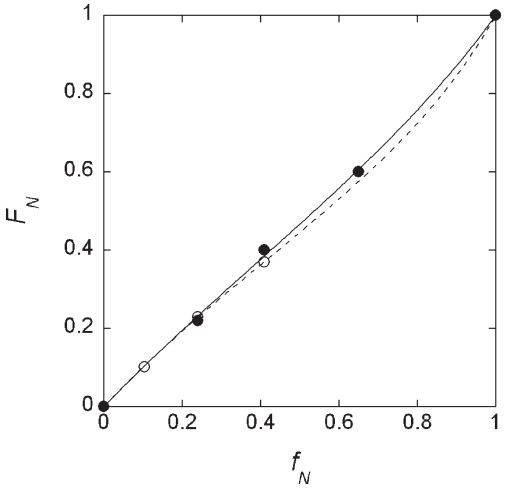


**Figure 3.** Mole fraction of N in the copolymer ($F_N$) as a function of the mole fraction of N in the feed ($f_N$) for the RAFT copolymerization of N and S. The filled circles are for the bulk copolymerization (condition 1), and the open circles are for solution polymerization (condition 2). The solid (condition 1) and dashed (condition 2) lines are nonlinear fits of the data according to eq 1.

different conditions: (1) bulk reaction under positive argon pressure and (2) solution reaction in toluene under reduced pressure. The mole fraction of N incorporated in the copolymer ($F_N$) as a function of mole fraction of N in the feed ($f_N$) is shown in Figure 3. We fit these data using the copolymerization equation (eq 1), where $r_N$ and $r_S$ are the reactivity ratios for N and styrene (S), respectively, and determine $r_N = 0.72$ and $r_S = 0.97$ (bulk), and $r_N = 0.56$ and $r_S = 0.94$ (solution). The fact that $r_N$ is somewhat greater than $r_S$ is consistent with the bulky norbornene substituent in N. The related radical copolymerization of the bulky *p*-*n*-decylstyrene styrene and styrene showed both reactivity ratios close to 1.[20]

$$F_N = \frac{f_N(r_N f_N + 1 - f_N)}{f_N(r_N f_N + 1 - f_N) + (1 - f_N)(r_S(1 - f_N) + f_N)} \quad (1)$$

*PLA-b-P(N-S) Block Copolymers.* With knowledge of the copolymerization kinetics of N and styrene, we prepared block copolymers employing a PLA-functional RAFT chain transfer agent (PLA-TC) that was previously reported.[7a] The synthetic scheme for PLA-*b*-P(N-*s*-S) copolymers is shown in Figure 4, and characterization of these block copolymers is summarized in Table 1.

SEC traces of the copolymers listed in Table 1 showed that these products exhibited narrow molecular weight distributions (Figures S3−S4 in the Supporting Information). However, a shoulder with twice the molecular weight of the main peak was apparent with increasing concentrations of N in the feed but became less prevalent at lower reaction temperatures, as in NSL(0.31). Additionally, no shoulder was observed in NSL(0) (i.e., no incorporation of N), so the high-molecular-weight peak in the SEC data was attributed to minor radical coupling

reaction of pendant norbornene groups. A related example illustrated that in a RAFT polymerization using a norbornene-containing initiator, coupling reaction from norbornene groups increased with reaction time.[23] DSC analysis of these copolymers showed two glass-transition temperatures ($T_g$): one corresponding to the PLA block at 52 °C and the other one corresponding to the P(N-S) block that varied with the N content in the P(N-S) block (Figure S5 in the Supporting Information), which is consistent with microphase segregation of PLA and P(N-S). A statistical (near random) distribution of pendant norbornene groups on PS backbone is expected, although compositional drift in the batch copolymerizations would lead to P(N-S) blocks with somewhat nonuniform composition distribution along the backbone. Overall, we were capable of producing well-defined norbornene-functional PLA-based copolymers with tailored contents of N and volume fractions of PLA.

*Small-Angle X-ray Scattering Analysis of PLA-b-P(N-s-S) copolymers*. We characterized the morphologies of the above PLA-*b*-P(N-S) copolymers using small-angle X-ray scattering (SAXS) (summarized in Table 1). The principal scattering peak observed corroborates microphase separation between the P(N-S) and PLA blocks, and higher order reflections infer long-range order. For instance, NSL(1) exhibited a cylindrical morphology (Figure S6 in the Supporting Information). We extracted the Flory−Huggins (F−H) interaction parameter, $\chi$, in these block copolymers with different norbornene compositions on the basis of the temperature dependence of the lamellar or cylindrical domain spacing in the strong-segregation regime ($\chi N > 100$) (eqs 2 and 3).[24] Although eqs 2 and 3 were derived for the strong-segregation regime, they have been used in the previous work to provide a reasonable estimation of $\chi$ for ordered lamellar and cylindrical block copolymers at moderate segregation strengths ($25 < N\chi < 85$).[25]

$$D_{lam} = 1.10aN^{2/3}\chi_{eff}^{1/6} \quad (2)$$

$$D_{cyl} = 1.12f^{1/6}(1+f^{1/2})^{2/3}aN^{2/3}\chi_{eff}^{1/6} \quad (3)$$

$$a = \left(\frac{f_{PLA}}{a_{PLA}^2} + \frac{f_{PNS}}{a_{PNS}^2}\right)^{-0.5} \quad (4)$$

For simplicity, we used the actual degree of polymerization for the number of statistical repeating units, $N$, in eqs 2 and 3 even though there would be some quantitative difference between these two values. The average statistical segment length, $a$, for the block copolymer was calculated using statistical segment lengths for PLA ($a_{PLA}$) and PS ($a_{PS}$) of 1.02 and 0.71 nm, respectively, on the basis of the segment volume of 185 Å$^3$, assuming that $a_{P(N-S)}$ was identical to that of PS.[6b] $f_{PLA}$ is the volume fraction of PLA, and $f_{P(N-S)}$ is the volume fraction of P(N-S) block. On the basis of SAXS measurements, we obtained the F−H parameter between the P(N-S) and PLA blocks, $\chi_{eff}$, by evaluating the principal domain spacing dependence on temperature (Figure S7 in the Supporting Information) using PLA-P(N-S) in entries 3, 4, and 6 of Table 1 with cylindrical morphologies and that in entry 8 with a lamellar morphology. In the previous work,[6] SAXS analysis of PS-*b*-PLA copolymers indicated $\chi_{PS/PLA} = 96.6/T - 0.091$; herein, we calculated $\chi_{PS/PLA} = 99.1/T - 0.111$ for NSL(0) using eq 2. For NSL(1) having a cylindrical morphology, we were able to obtain $\chi_{PN/PLA} = 199.1/T - 0.174$ using eq 3. The incorporation of hydrophobic pendant norbornene groups led to an approximately two-fold increase in segregation strength compared with PS-PLA. Furthermore, the segregation strength between PLA and P(N-S) blocks can be tailored by the level of N incorporation. The group contributions to solubility parameter (Hoy values),[26] $\delta$(PLA) = 20 and $\delta$(PN) = 16.4 MPa$^{1/2}$, give rise to a calculated $\chi_{PN/PLA}$ of $181/T$ using a reference volume of 185 Å$^3$, which is in reasonable agreement with the SAXS results.

**Self-Assembly of PLA-*b*-P(N-S)/DCPD Composites and Fabrication of Nanoporous Monoliths.** *Self-Assembly of PLA-b-P(N-S) and DCPD*. In addition to the study of the bulk morphology of block copolymers, self-assembly of block copolymers with a selective solvent has captured much attention.[27] For instance, PS-*b*-PI (15−13 kg mol$^{-1}$) in a PS-selective solvent diethyl phthalate can adopt various morphologies, such as spheres, cylinders, and lamellae depending on the composition of the solvent.[27a] Using a selective solvent that can cross-link with the solvent-philic block, we anticipated improvements in not only thermal and mechanical properties of the composites but also the ability

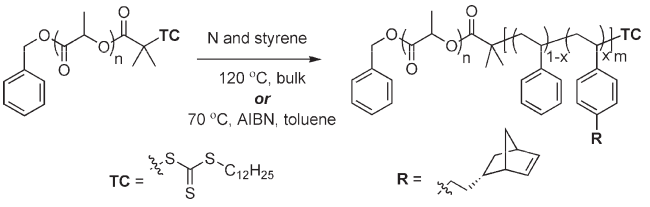


**Figure 4.** Synthetic scheme of PLA-*b*-P(N-S) copolymers.

**Table 1. Summary of PLA-*b*-P(N-S) Synthesized by RAFT Polymerization**

| entry | polymer[a] | $M_n$ (SEC) (kg mol$^{-1}$) | PDI | $M_n$ (NMR) (kg mol$^{-1}$)[b] | $f_{PLA}$ (%)[c] | $T_g$ (PNS) (°C) | N molar ratio | | morphology at 140 °C |
|---|---|---|---|---|---|---|---|---|---|
| | | | | | | | feed | polymer | |
| 0 | PLATC | 13.7 | 1.09 | 10.6 | | | | | |
| 1 | NSL(0.11) | 23.1 | 1.27 | 23.6 | 39.4 | 90 | 0.10 | 0.11 | C + L |
| 2 | NSL(0.23) | 23.6 | 1.26 | 23.0 | 40.5 | 86 | 0.24 | 0.23 | C + L |
| 3 | NSL(0.44) | 23.2 | 1.37 | 23.0 | 40.5 | 82 | 0.41 | 0.44 | C |
| 4 | NSL(0.67) | 22.4 | 1.34 | 22.4 | 41.7 | 79 | 0.65 | 0.67 | C |
| 5 | NSL(0.46) | 19.9 | 1.17 | 19.2 | 49.3 | 78 | 0.41 | 0.46 | L |
| 6 | NSL(1) | 21.4 | 1.19 | 21.4 | 43.8 | 76 | 1.00 | 1.000 | C |
| 7 | NSL(0.31) | 21.3 | 1.20 | 21.2 | 44.3 | 83 | 0.32 | 0.31 | L |
| 8 | NSL(0) | 21.4 | 1.17 | 21.3 | 44.0 | 90 | 0 | 0 | L |

[a] Entries 1−5 were synthesized from PLATC, styrene, and N at 120 °C for 4 h via thermal initiation (Experimental Section), whereas entries 6−8 were prepared in toluene for 20 h at 70 °C initiated by 2,2'-azodiisobutyronitrile. For NSL($x$), NSL represents the PLA-*b*-P(N-S) copolymer and $x$ denotes the molar ratio of N in the P(N-S) block. [b] From the NMR analysis, molecular weight of the TC was included in all $M_n$ calculations, and in entry 0, $M_n$ (PLAOH) = 10.3 kg mol$^{-1}$. [c] To calculate the PLA volume fraction, the TC group was included as a part of the PNS block, and $f_{PLA}$ was based on densities of polymers at 140 °C: $\rho$(PS) = 0.97 g cm$^{-3}$,[21] $\rho$(PLA) = 1.154 g cm$^{-3}$,[22] and assuming $\rho$(PN) = $\rho$(PS).

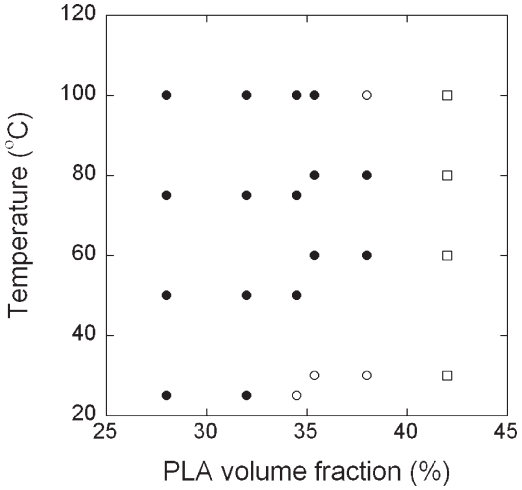


**Figure 5.** Partial morphology map for NSL(0.46)/DCPD blends at different temperatures from SAXS experiments. Filled circles denote cylindrical morphology, and open circles and squares represent lamellar and unidentified morphologies, respectively. The volume fraction of PLA was calculated assuming that densities of PLA and the matrix phase are 1.254[22] and 1.0 g/cm$^3$ at room temperature.

to tailor the blend morphology. For the purposes of cross-linking P(N-S) with DCPD using metathesis reactions, the self-assembly of DCPD and PLA-*b*-P(N-S) mixtures must be addressed. A waxy solid composed of NSL(0.11) (entry 1 in Table 1) and DCPD at a mass ratio of 2:1 was prepared. (See the Experimental Section.) DSC analysis of this waxy solid (Figure S8 in the Supporting Information) indicated clear shift of $T_g$ to lower temperatures in both PLA and PNS domains compared with NSL(0.11). Using the Fox equation,[28] we determined two independent variables: a hypothetical $T_g$ of DCPD and fraction of DCPD in both PLA and P(N-S) domains. We concluded that DCPD was distributed in the PLA and P(N-S) domains at a ratio of 1 to 4, which is in agreement with the anticipated distribution based on the structural similarity between P(N-S) and DCPD.

NSL(0.46) adopts a lamellar morphology (entry 5 in Table 1) and was chosen to study the morphology of assembled PLA-*b*-P(N-S)/DCPD mixtures and for subsequent cross-linking reactions. PLA-*b*-P(N-S)/DCPD blends with different PLA volume factions were prepared using the procedure described in the Experimental Section. The blend composition was determined by $^1$H NMR spectroscopy. For SAXS analysis, the waxy solid was sandwiched between Kapton films in a rubber O-ring, assuming that DCPD evaporation below 100 °C was negligible during experiment. A wide region of the cylindrical morphology is evident over a range of temperatures in Figure 5; the introduction of DCPD in the P(N-S) phase drives the phase transition from lamellae to hexagonally packed cylinders, which is the targeted phase for our subsequent cross-linking studies. The 1D SAXS profiles of a NSL(0.46)/DCPD blend ($f_{PLA}$ = 30% by volume) that adopts a cylindrical morphology are shown in Figure S9 in the Supporting Information.

*Nanoporous Monoliths from PLA*-b-*P(N-S)/DCPD*. To produce nanoporous monoliths, a NSL(0.46)/DCPD blend with a PLA volume fraction of around 30% was prepared. The incorporation of a metathesis catalyst to the blend resulted in gelation within minutes at room temperature before removal of the cosolvent used for sample preparation. This problem was overcome by the addition of $PPh_3$ to attenuate the catalyst reactivity.[29]

In a NSL(0.46)/DCPD blend containing 0.25 wt % of the first generation Grubbs catalyst and 0.75 wt % $PPh_3$, the $^1$H NMR spectrum indicated a negligible cross-linking reaction in the resultant waxy orange solid before curing. Less than 5 wt % residual $CH_2Cl_2$ was in the blend, and the DCPD content before cross-linking was 60 wt % relative to the copolymer. We expected a cylindrical morphology given the calculated weight fraction of PLA ($f_{PLA}$) of 33.5 wt % in this composite (corresponding PLA volume fraction of PLA of 29% at room temperature, see Figure 5). The waxy solid was pressed using a homemade channel die[6b] at 60 °C (to facilitate processing) within 5 min of its preparation to align the PLA cylinders in the flow direction. Finally, the blend was cured in a small tube under argon at 70 °C for 12 h and at 110 °C for 3 h. After cross-linking, slight mass loss of the blend was apparent because of DCPD evaporation. SAXS analysis indicated that the initial cylindrical morphology was maintained during and after cross-linking.

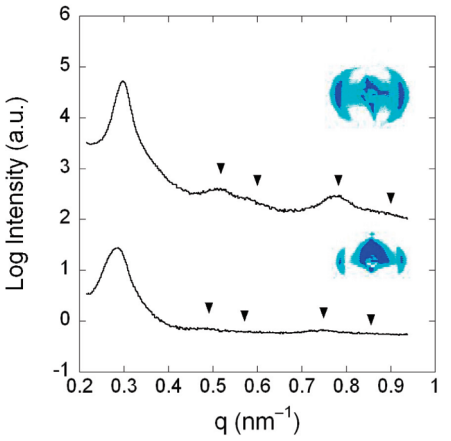


**Figure 6.** SAXS profiles of cross-linked monoliths before (bottom) and after PLA removal (top). Higher order peaks relative to the primary peak located at $\sqrt{3}$, $\sqrt{4}$, $\sqrt{7}$, and $\sqrt{9}$ indicate a cylindrical morphology.

After degradation of PLA (Experimental Section), IR spectra (Figure S10 in the Supporting Information) showed the disappearance of the resonance at 1750 cm$^{-1}$ corresponding to C=O stretching, which indicated nearly complete removal of the PLA phase in the cross-linked monoliths. The monoliths lost about 35 wt % of their mass following PLA degradation, which is slightly higher than the mass fraction of PLA in the composite. The 2D SAXS data (Figure 6) of the cross-linked samples showed two broad reflections consistent with cylinder orientation in the flow direction. The degree of alignment in nanoporous monoliths was characterized by the second-order orientation factor, $F_2$, of 0.8.[6b] After PLA removal, the scattering intensity in the monoliths exhibited a 27-fold increase, which was consistent with the anticipated increase in electron density contrast for a nanoporous sample.[16] The slight shift of the primary peak (q*) after PLA removal to a higher value indicated the slight decrease in the domain size, which was likely attributed to the slight shrinkage of the cross-linked matrix following PLA hydrolysis. The domain spacing from SAXS of 21.1 nm gave a PLA domain size (pore size) of about 13.8 nm on the basis of the pore volume fraction of 29%.

Figure 7 and Figure S11 in the Supporting Information are typical SEM images for fractured surfaces of monoliths in two directions: parallel to and normal to the cylinder axis, confirming a structure with an array of hexagonally packed cylindrical pores. The pore diameter determined from the SEM image is 11 ± 2 nm (accounting for 1 nm Pt coating). The averaged domain spacing was about 21 ± 2 nm, which is consistent with the SAXS analysis. In $N_2$ adsorption experiments, the Brunauer−Emmett−Teller (BET) analysis

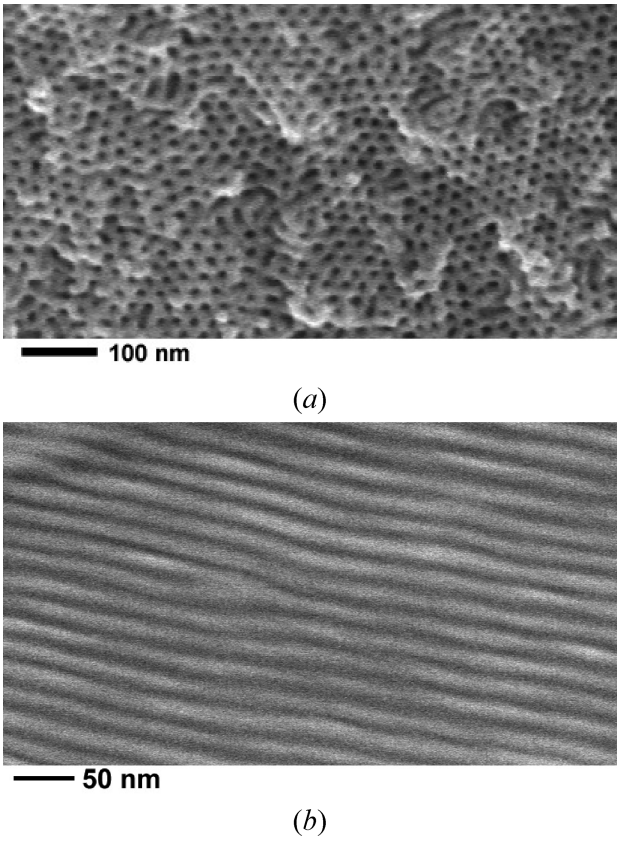


**Figure 7.** SEM images of cross-linked nanoporous monoliths fractured in two directions: (a) normal to the channel axis and (b) parallel to the channel axis. Samples were cryofractured and coated with 1 nm Pt via direct sputtering to prevent charging.

shows a type IV isotherm and gave a specific surface area of 132 $m^2$ $g^{-1}$. Analysis of the desorption data gave an average pore diameter of 9 nm and a peak width at half height of 3 nm (Figure 8). Barrett−Joyner−Halenda (BJH) analysis gave an average pore diameter of 12.5 nm, which is in agreement with SEM data.[30] The pore diameter calculated from the SAXS data (13.8 nm) was somewhat higher than that determined by both SEM and $N_2$ adsorption analysis. We suspect this was due to inaccuracies in the estimated density of poly(DCPD)/PS matrix.

In previously reported nanoporous PS monoliths, an exothermic peak in the initial heating trace of the DSC analysis corresponded to the collapse of nanopores above the $T_g$ of PS (100 °C).[6b] In the polyDCPD composite monoliths described here, no detectable thermal transition appeared in the DSC thermogram up to 130 °C (Figure S12 in the Supporting Information). Furthermore, the nanoporous structure was preserved after heating to 130 °C according to SEM. However, substantial pore collapse was evident after annealing the nanoporous monoliths at 150 °C for 1 h, presumably due to the softening of the polyDCPD-containing matrix.[15] The solvent resistibility of these monoliths was examined by immersion in THF, where the THF-swollen monoliths were soaked in methanol, allowing for plasticization of the polyDCPD-containing matrix before drying, and SEM analysis confirms preservation of the nanoporous structure (Figure S13c in the Supporting Information). SAXS analysis of nanoporous monoliths after the aforementioned thermal (130 °C) and solvent treatments gave comparable scattering intensities that are typical for untreated nanoporous samples that also consistent with preservation of porosity.

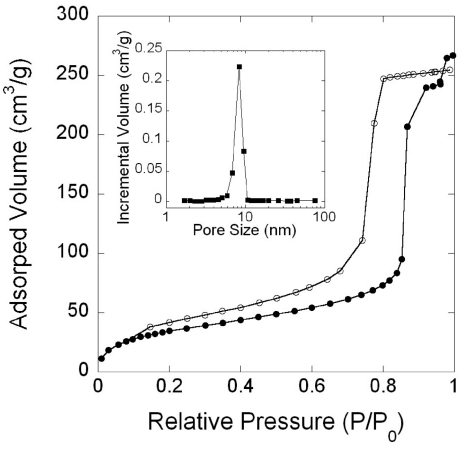


**Figure 8.** Nitrogen adsorption (solid) and desorption (open) isothermal curves of the nanoporous monoliths. Inset: pore size distribution calculated from the desorption process.

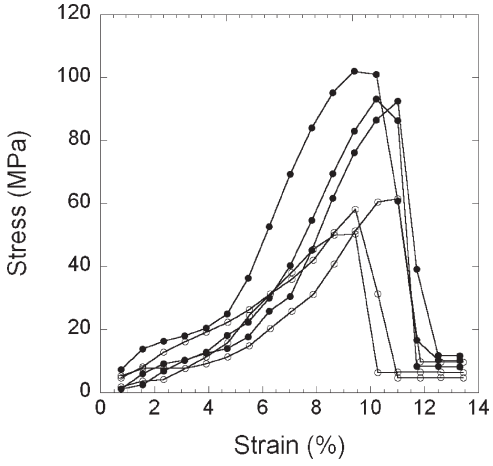


**Figure 9.** Tensile testing of cross-linked monoliths before (solid) and after (open) PLA degradation.

The mechanical properties of the composite nanoporous monoliths were evaluated by tensile testing with extension parallel to the channel direction (Figure 9). The average tensile strength of resulting cross-linked samples (ca. 90 MPa) was higher than pure cross-linked polyDCPD plastics (55 MPa), which was likely attributed to higher cross-linking density by incorporation of the reactive P(N-S) blocks. For the nanoporous samples, the average elongation at break was about 10%, and the average tensile strength was about 50 MPa, which is significantly improved in comparison with un-cross-linked nanoporous PS that was too brittle to be appropriately loaded in the same test.

## Conclusions

In conclusion, a new norbornene-functional styrene monomer was prepared, and the synthesis of PLA-*b*-P(N-S) block copolymers containing tailored norbornene functionality was demonstrated. DSC and SAXS analysis of these materials confirmed that these block polymers adopted morphologies consistent with their compositions. We demonstrated the fabrication of cylindrically nanoporous monoliths via metathesis cross-linking in a preassembled reactive blend containing DCPD templated by block copolymers, which have excellent thermal and mechanical stability and solvent resistance. This approach shows the utility of metathesis chemistry to generate robust nanoporous materials, which are potentially favorable for catalyst supports and other applications.

## Experimental Section

**Materials.** Unless specifically noted, all chemicals were purchased from Aldrich and used without further purification. Styrene was passed through basic alumina and then distilled over calcium hydride under reduced pressure. Degassed toluene (HPLC grade) was purified by passage through a home-built solvent purification system equipped with activated alumina and a supported copper catalyst to remove traces of protic impurities; THF (HPLC grade) was degassed under nitrogen and passed through a home-built solvent purification system equipped with activated alumina.[31] Radical inhibitors in 4-chloromethylstyrene were removed by passage through a short basic alumina column. D,L-lactide was recrystallized from ethyl acetate and dried under vacuum at room temperature. *S*-1-Dodecyl-*S*′-(α,α′-dimethyl-α″-acetic acid) trithiocarbonate (CTA) was prepared using a reported procedure.[32]

**General Characterization.** All NMR spectra were recorded on a Varian VI-300 spectrometer using deuterated chloroform (Cambridge). SEC data were collected using a Hewlett-Packard 1100 series liquid chromatograph equipped with Jordi polydivinylbenzene columns with pore sizes of 10 000, 1000, and 500 Å as well as a Hewlett-Packard 1047A refractive index detector. THF was used as the mobile phase at 40 °C with a flow rate of 1 mL/min. The SEC instrument was calibrated with PS standards (Polymer Laboratories). DSC analyses were performed on a TA Q1000 instrument using a scan rate of 20 °C/min, and glass-transition temperatures were recorded from the second heating trace. Mass spectrometry (MS) was performed on a Finnigan MAT 95 instrument with the sample introduced by a Hewlett-Packard Series II model 5890 gas chromatograph (GC). SAXS profiles were recorded on a 230 cm custom-built beamline at the University of Minnesota. Cu Kα X-rays ($\lambda$ = 1.542 Å) were generated through a Rigaku RU-200BVH rotating anode fitted with a 0.2 × 2 $mm^2$ microfocus cathode and Franks mirror optics. The sample was equilibrated under helium purge for 5 min at each temperature before collection. Two-dimensional diffraction patterns were recorded using a Siemens area detector and were corrected for detector response before analysis. The 2D images were azimuthally integrated to a 1D plot of intensity versus $q$, where $q = 4\pi/\lambda \sin(\theta/2)$ and $\theta$ and $\lambda$ are the scattering angle and X-ray wavelength, respectively. SEM images were obtained on a Hitachi S-900 FE-SEM instrument using a 3.0 kV accelerating voltage. Prior to SEM analysis, fractured monoliths were coated with a 1.0 nm thick Pt layer via direct Pt sputtering. Fourier transform infrared (FT-IR) spectrometry was conducted on a Nicolet Magna-IR spectrometer 550, and the liquid sample was placed between NaCl plates, whereas solid samples were grounded with KBr and subsequently pressed into transparent thin films. The $N_2$ adsorption experiment was performed on a Micromeritics ASAP 2000 instrument, and samples were degassed under high vacuum overnight at 60 °C. Tensile tests of monolithic bars (10 × 2 × 1 $mm^3$) were carried out on a Rheometric Scientific MINIMAT instrument at room temperature, operating at a crosshead speed of 2 mm/min with a load cell of 1000 N.

**Synthesis of *p*-Norbornenylethyl Styrene.** 5-Bromomethyl norbornene was prepared following a literature procedure.[33] Norbornenylethyl styrene (N) was prepared using a modified route:[34] 5-bromomethyl norbornene (4.42 g, 23.5 mmol) was added dropwise to magnesium powders (0.65 g, 27 mmol) in anhydrous THF (25 mL) and reacted at 40 °C for 16 h. The as-formed Grignard reagent in THF was isolated from the excess magnesium and was added dropwise to a solution of 4-chloromethylstyrene (3.04 g, 20 mmol) in anhydrous THF (15 mL) with $Li_2CuCl_4$ solution (3 mL, 0.1 M in THF) at −78 °C under argon. The reaction solution was kept at −78 °C for 6 h and then warmed to room temperature. The solution was quenched with saturated aqueous $NH_4Cl$ and extracted with diethyl ether twice. The combined ether phase was washed with saturated $Na_2CO_3$ aqueous solution and brine and dried over $MgSO_4$. After the removal of $MgSO_4$, the concentration under reduced pressure yielded a pale-yellow oil. Purification of this crude product by column chromatography (silica, hexanes) afforded a colorless oil (3 g). $^1$H NMR spectrum of N (majority: the endo isomer), $\delta$: 7.35(d, 2H, $J$ = 10.4 Hz, Ar*H*), 7.15 (d, 2H, $J$ = 10.1 Hz, Ar*H*), 6.72 (t, 1H, $J$ = 17.4, 10.6 Hz, −C*H*=$CH_2$), 6.06−6.19 (m, 2H, −C*H*=C*H*−), 5.73 (1H, d, $J$ = 17.7, −CH=C$H_2$), 5.21 (d, 1 H, $J$ = 10.8, −CH=C$H_2$), 2.81 (d, 2H, $J$ = 10.8, −C*H*−CH=CH−C*H*−), 2.61 (t, 2H, $J$ = 8.0 Hz, Ar−C$H_2$−), 1.99−2.08 (m, 1H, −C*H*−$CH_2$−$CH_2$−Ar), 1.89 (m, 1H, −CH−C$H_2$(exo)−CH−), 1.36−1.50 (m, 3H, −CH−C$H_2$−CH− and −C$H_2$−$CH_2$−Ar), 1.24 (d, 1H, $J$ = 8.4 Hz, −CH−C$H_2$−CH−), 0.57 (m, 1H, −CH−C$H_2$(endo)−CH−). $^{13}$C NMR of *endo*-N (75 MHz): 142.9, 137.2, 136.8, 135.1, 132.4, 128.6, 126.2, 112.9, 49.7, 45.4, 42.7, 38.4, 36.7, 35.0, 32.5. MS: 224.2 (M+), 66 ($C_5H_6$+), 117.1 ($C_2H_3$−Ph−CH+), 158.1 ($C_2H_3$−Ph−$CH_2CH_2$CH=$CH_2$+). FT-IR ($cm^{-1}$): (stretching) C=C, 1630, 1610; ArH, 1570, 1510, 1450; −C−H, 2870, 2970; =C−H, 3060, 3080; (vibrating of =C−H) the vinyl group, 990, 904; *p*-substituted benzene, 830; norbornene, 717. Elemental analysis: C 90.70% and H 9.16% (found); C 91.01% and H 8.99% (calculated).

**Kinetics Study in Copolymerization.** Condition 1: CTA (3.5 mg) and styrene and N (in total 0.5 mL at different ratios) were placed in a 10 mL reactor and sealed under Ar pressure after three freeze−pump−thaw cycles. Condition 2: CTA (3.5 mg), dry toluene (0.5 mL), and styrene and N (in total 0.5 mL at different ratios) were placed in a 10 mL reactor and sealed under vacuum after three freeze−pump−thaw cycles. Under these conditions, styrene vaporization during polymerization that resulted in increasing $f_N$ could be ignored. Polymerization reactions were conducted at 120 °C for 1 to 2 h, where the reaction time was increased with decreasing N concentrations in feed. The final monomer conversion was between 3 and 6 wt % on the basis of the recovered polymers by precipitation in methanol and molecular weight by NMR spectroscopy. Molar ratios in feed were calculated using $\rho$(styrene) and $\rho$(N) = 0.9 g $mL^{-1}$ at 25 °C, whereas molar ratios in the polymer were calculated from the NMR spectra.

**Synthesis of PLA-*b*-P(N-S) and PLA-*b*-PN.** PLA-attached chain transfer agent (PLATC) was synthesized according to an established procedure.[7a] PLATC (0.2 g, 0.019 mmol, $M_n$ = 10.6 kg/mol, PDI = 1.09) and monomer N and styrene (total volume of 1.0 mL, except for entry 5 in Table 1 with total volume of 0.8 mL) at different ratios were mixed in an air-free flask, followed by three freeze−pump cycles, sealed under vacuum, and finally reacted at 120 ± 1 °C for 4 h. Besides the bulk condition, three polymerization reactions were carried out in toluene as follows: PLATC (0.2 g, 0.019 mmol), N and styrene (1.0 mL), and AIBN (0.35 mg, 0.002 mmol) were dissolved in toluene (1.0 mL) in an air-free flask, followed by three freeze−pump−thaw cycles, and reacted at 70 °C for 20 h. Resultant copolymers were recovered through precipitation in methanol, followed by dissolution in $CH_2Cl_2$ and reprecipitation in pentane and finally dried under vacuum. The overall monomer conversion was between 20 and 30 wt % determined using NMR analysis. $^1$H NMR spectrum of PLA-*b*-P(N-*s*-S), $\delta$: 6.2−7.2 (b, Ar*H*), 5.9−6.2 (b, −C*H*=C*H*−), 5.1−5.3 (b, −C(O)−C*H*-($CH_3$)−O−), 2.8 (b, −C*H*−CH=CH−C*H*−), 2.55 (b, Ar−C$H_2$−), 2.0 (b, −C*H*−$CH_2$−$CH_2$−Ar), 1.86 (b, −CH−C$H_2$(exo)−CH−), 1.39 (b, −CH−C$H_2$−CH− and −C$H_2$−$CH_2$−Ar), 1.25 (d, −CH−C$H_2$−CH−), 0.55 (b, −CH−C$H_2$(endo)−CH−).

**General Procedure for Preparing Cross-Linked Nanoporous Monoliths.** PLA-*b*-P(N-S) (0.2 g) and DCPD (0.1 to 0.2 g) were predissolved in $CH_2Cl_2$ (1.5 mL), and most $CH_2Cl_2$ and part of DCPD were removed under reduced pressure for some time between 10 to 30 min. Precise composition in the resultant blend

was determined through NMR analysis. For the cross-linking procedure, the first generation Grubbs catalyst (0.9 mg) with $PPh_3$ (2.7 mg) dissolved in $CH_2Cl_2$ (0.2 mL) was added to a homogeneous copolymer (0.2 g)/DCPD (0.16 g) solution and stirred for 20 s. Most $CH_2Cl_2$ and part of DCPD were removed under vacuum for about 20 min to a desired blend composition (e.g., $f_{PLA}$ = 29% by volume). Next, the waxy mixture was pressed into a thin film at room temperature between two Teflon films, carefully peeled off Teflon by soaking in liquid $N_2$, and then hot-pressed through a homemade channel die at 70 °C to form long rectangular bars. (Cylindrical PLA domains were aligned in the flow direction.) The aligned samples were placed in a sealed pressure vessel under positive argon pressure and cured at 70 °C for 12 h and annealed at 110 °C for 3 h. The cross-linked monoliths were dried under vacuum overnight before analysis. Finally, we etched the PLA phase in these cross-linked samples by placing monolithic samples in NaOH solution (a 4:6 (v/v) mixture of methanol and water) for 7 days at 70 °C in an oil bath. Resulting nanoporous monoliths were subsequently rinsed with water and MeOH and dried under vacuum at 60 °C for 2 days before further analysis.

**Acknowledgment.** This work was supported by the U.S. Department of Energy through grant 5-35908. Parts of this work were carried out in the University of Minnesota I.T. Characterization Facility, which receives partial support from NSF through the NNIN program. We thank Mark Amendt and Louis Pitet for helpful input.

**Supporting Information Available:** $^1H$ NMR spectra of monomer N and corresponding polymer PN, $^{13}C$ NMR spectra of monomer N, SEC curves of PLA-*b*-P(N-*s*-S) produced from RAFT copolymerization in toluene, DSC traces of PLA-*b*-P(N-*s*-S) copolymers, SAXS profiles of copolymer NSL(1), effective Flory−Huggins parameters $\chi_{eff}$ in PLA-*b*-P(N-*s*-S) copolymers, DSC traces of NSL (0.11) and a NSL (0.11)/DCPD blend, temperature-dependent SAXS profiles of a NSL(0.46)/DCPD blend in a cylindrical morphology, IR spectra of cross-linked monoliths before and after PLA removal, SEM images of fractured mesoporous monoliths, DSC analysis of crosslinked monoliths before and after PLA removal, and SEM images of fractured mesoporous surfaces. This material is available free of charge via the Internet at http://pubs.acs.org.

## References and Notes

(1) For two reviews see: (a) Hillmyer, M. A. *Adv. Polym. Sci.* **2005**, *190*, 137–181. (b) Olson, D. A.; Chen, L.; Hillmyer, M. A. *Chem. Mater.* **2008**, *20*, 869–890.
(2) (a) Park, M.; Harrison, C.; Chaikin, P. M.; Register, R. A.; Adamson, D. H. *Science* **1997**, *276*, 1401–1404. (b) Chan, V. Z.-H.; Hoffman, J.; Lee, V. Y.; Iatrou, H.; Avgeropoulos, A.; Hadjichristidis, N.; Miller, R. D.; Thomas, E. L. *Science* **1999**, *286*, 1716–1719. (c) Thurn-Albrecht, T.; Steiner, R.; DeRouchey, J.; Stafford, C. M.; Huang, E.; Bai, M.; Tuominen, M.; Hawker, C. J.; Russell, T. P. *Adv. Mater.* **2000**, *12*, 787–791.
(3) Thurn-Albrecht, T.; Schotter, J.; Kastle, G. A.; Emley, N.; Shibauchi, T.; Krusin-Elbaum, L.; Guarini, K.; Black, C. T.; Tuominen, M. T.; Russell, T. P. *Science* **2000**, *290*, 2126–2129.
(4) (a) Yang, S. Y.; Ryu, I.; Kim, H. Y.; Kim, J. K.; Jang, S. K.; Russell, T. P. *Adv. Mater.* **2006**, *18*, 709–712. (b) Phillip, W. A.; Rzayev, J.; Hillmyer, M. A.; Cussler, E. L. *J. Membr. Sci.* **2006**, *286*, 144–152.
(5) (a) Walheim, S.; Schaffer, E.; Mlynek, J.; Steiner, U. *Science* **1999**, *283*, 520–522. (b) Joo, W.; Park, M. S.; Kim, J. K. *Langmuir* **2006**, *22*, 7960–7963.
(6) (a) Zalusky, A. S.; Olayo-Valles, R.; Taylor, C. J.; Hillmyer, M. A. *J. Am. Chem. Soc.* **2001**, *123*, 1519–1520. (b) Zalusky, A. S.; Olayo-Valles, R.; Wolf, J. H.; Hillmyer, M. A. *J. Am. Chem. Soc.* **2002**, *124*, 12761–12773.
(7) (a) Rzayev, J.; Hillmyer, M. A. *J. Am. Chem. Soc.* **2005**, *127*, 13373–13379. (b) Bailey, T. S.; Rzayev, J.; Hillmyer, M. A. *Macromolecules* **2006**, *39*, 8772–8781. (c) Mao, H.; Arrechea, P. L.; Bailey, T. S.; Johnson, B. J. S.; Hillmyer, M. A. *Faraday Discuss.* **2005**, *128*, 149–162.
(8) Johnson, B. J. S.; Wolf, J. H.; Zalusky, A. S.; Hillmyer, M. A. *Chem. Mater.* **2004**, *16*, 2909–2917.
(9) Wolf, J. H.; Hillmyer, M. A. *Langmuir* **2003**, *19*, 6553–6560.
(10) (a) Drockenmuller, E.; Li, L. Y. T.; Ryu, D. Y.; Harth, E.; Russell, T. P.; Kim, H.-C.; Hawker, C. J. *J. Polym. Sci., Part A: Polym. Chem.* **2005**, *43*, 1028–1037. (b) Leiston-Belanger, J. M.; Russell, T. P.; Drockenmuller, E.; Hawker, C. J. *Macromolecules* **2005**, *38*, 7676–7683.
(11) (a) Cavicchi, K. A.; Zalusky, A. S.; Hillmyer, M. A.; Lodge, T. P. *Macromol. Rapid Commun.* **2004**, *25*, 704–709. (b) Hansen, M. S.; Vigild, M. E.; Berg, R. H.; Ndoni, S. *Polym. Bull.* **2004**, *51*, 403–409.
(12) Guo, F.; Andreasen, J. W.; Vigild, M. E.; Ndoni, S. *Macromolecules* **2007**, *40*, 3669–3675.
(13) Zhou, N.; Bates, F. S.; Lodge, T. P. *Nano. Lett.* **2006**, *6*, 2354–2357.
(14) Uehara, H.; Yoshida, T.; Kakiage, M.; Yamanobe, T.; Komoto, T.; Nomura, K.; Nakajima, K.; Matsuda, M. *Macromolecules* **2006**, *39*, 3971–3974.
(15) Kelsey, D. R.; Chuan, H. H.; Ellison, R. H. *J. Polym. Sci., Part A: Polym. Chem.* **1997**, *35*, 3049–3063.
(16) Chen, L.; Phillip, W. A.; Cussler, E. L.; Hillmyer, M. A. *J. Am. Chem. Soc.* **2007**, *129*, 13786–13787.
(17) Hirao, A.; Loykulnant, S.; Ishizone, T. *Prog. Polym. Sci.* **2002**, *27*, 1399–1471.
(18) Wang, Y.; Hillmyer, M. A. *Macromolecules* **2000**, *33*, 7395–7403.
(19) Chiefari, J.; Chong, Y. K.; Ercole, F.; Krstina, J.; Jeffery, J.; Le, T. P. T.; Mayadunne, R. T. A.; Meijs, G. F.; Moad, C. L.; Moad, G.; Rizzardo, E.; Thang, S. H. *Macromolecules* **1998**, *31*, 5559–5562.
(20) Buckley, D. A.; Augostini, P. P. *J. Appl. Polym. Sci.* **1979**, *23*, 311–314.
(21) Fetters, L. J.; Lohse, D. J.; Richter, D.; Witten, T. A.; Zirkel, A. *Macromolecules* **1994**, *27*, 4639–4647.
(22) Witzke, D. R.; Narayan, R.; Kolstad, J. J. *Macromolecules* **1997**, *30*, 7075–7085.
(23) Patton, D. L.; Advincula, R. C. *Macromolecules* **2006**, *39*, 8674–8683.
(24) (a) Leibler, L. *Macromolecules* **1980**, *13*, 1602–1617. (b) Matsen, M. W.; Bates, F. S. *J. Chem. Phys.* **1997**, *106*, 2436–2448.
(25) Ren, Y.; Lodge, T. P.; Hillmyer, M. A. *Macromolecules* **2002**, *35*, 3889–3894.
(26) Du, Y.; Xue, Y.; Frisch, H. L. In *Physical Properties of Polymers Handbook*; Mark, J. E., Ed.; AIP Press: Woodbury, NY, **1996**; Chapter 16, p 232.
(27) (a) Lodge, T. P.; Pudil, B.; Hanley, K. J. *Macromolecules* **2002**, *35*, 4707–4717. (b) Lai, C.; Russel, W. B.; Register, R. A. *Macromolecules* **2002**, *35*, 841–849. (c) Ding, J.; Carver, T. J.; Windle, A. H. *Comp. Theo. Polym. Sci.* **2001**, *11*, 483–490.
(28) Couchman, P. R. *Macromolecules* **1978**, *11*, 1156–1161.
(29) Sanford, M. S.; Love, J. A.; Grubbs, R. H. *J. Am. Chem. Soc.* **2001**, *123*, 6543–6554.
(30) Gregg, S. J.; Sing, K. S. W. *Adsorption, Surface Area and Porosity*; Academic Press: London, **1982**.
(31) Pangborn, A. B.; Giardello, A.; Grubbs, R. H.; Rosen, R. K.; Timmers, F. J. *Organometallics* **1996**, *15*, 1518–1520.
(32) Lai, J. T.; Filla, D.; Shea, R. *Macromolecules* **2002**, *35*, 6754–6756.
(33) Dolman, S. J.; Hultzsch, K. C.; Pezet, F.; Teng, X.; Hoveyda, A. H.; Schrock, R. R. *J. Am. Chem. Soc.* **2004**, *126*, 10945–10953.
(34) Stubbs, L. P.; Weck, M. *Chem.—Eur. J.* **2003**, *9*, 992–999.